

A new polysaccharide from *Caulerpa chemnitzia* induces molecular shifts of immunomodulation on macrophages RAW264.7

Yulin Wu^{a,1}, Jun Liu^{b,1}, Huili Hao^a, Lianmei Hu^c, Xiaoyong Zhang^d, Lianxiang Luo^b, Jincheng Zeng^b, Wei Zhang^e, Io Nam Wong^e, Riming Huang^{a,*}

^a Guangdong Provincial Key Laboratory of Food Quality and Safety, College of Food Science, South China Agricultural University, Guangzhou 510642, China

^b Laboratory of Pathogenic Biology, The Marine Biomedical Research Institute, Dongguan Key Laboratory of Medical Bioactive Molecular Developmental and Translational Research, Guangdong Medical University, Zhanjiang, Guangdong 524023, China

^c College of Veterinary Medicine, South China Agricultural University, Guangzhou 510642, China

^d Joint Laboratory of Guangdong Province and Hong Kong Region on Marine Bioresource Conservation and Exploitation, College of Marine Sciences, South China Agricultural University, Guangzhou 510642, China

^e State Key Laboratory of Quality Research in Chinese Medicines and Macau Institute for Applied Research in Medicine and Health, Faculty of Medicine, Macau University of Science and Technology, Taipa, Macau 999078, China

ARTICLE INFO

Keywords:

Caulerpa chemnitzia
Polysaccharide
Immunomodulatory effect
Transcript-metabolic analysis
NF- κ B signaling pathway
Arachidonic acid metabolism pathway

ABSTRACT

Investigation on *Caulerpa chemnitzia* polysaccharides led to the finding of a new polysaccharide (CCP). The basic components of CCP were the total sugar ($59.18\% \pm 0.57\%$), the uronic acids ($36.75\% \pm 0.28\%$) and the sulfate ($42.50\% \pm 0.42\%$), in total content. The physicochemical analysis revealed that CCP was a heteropolysaccharide with a molecular weight of 321.6 KDa, and composed of arabinose, fucose, glucose, mannose, galactose, xylose, fructose, ribose, glucuronic acid and galacturonic acid. The immunomodulatory assay showed that CCP played an important role in activating cell viability, the nitric oxide product and cytokines (IL-6 and TNF- α) secretion. Furthermore, the transcript-metabolic analysis displayed a total of 7692 differentially expressed genes (DEGs) and 95 differentially accumulated metabolites (DAMs), and revealed that CCP may play an immunomodulatory effect by activating NF- κ B signaling pathway and arachidonic acid metabolism pathway. These findings will provide a basic understanding to further investigation of *Caulerpa* polysaccharides.

Introduction

Polysaccharides are highly polymerized carbohydrate composed of more than ten monosaccharides linked by glycoside bonds. Polysaccharides are widely distributed in nature and considered as an important research object. As algae are important marine resources with of a great variety of polysaccharides. Recently, due to their various biological activities, natural polysaccharides extracted from marine algae have attracted researchers' attention such as *Porphyra haitanensis* polysaccharide with antioxidant and immunostimulatory activities (Gong et al., 2020), *Ulvan suppresses* polysaccharide with antitumor and immunoregulatory activities (Zhao et al., 2020), *Ulva pertusa* polysaccharide with antiviral activity (Chi, Zhang, Wang, Fu, Guan, & Wang,

2020), *Chaetomorpha linum* polysaccharide with anticoagulant activity (Qin et al., 2020), *Gracilaria lemaneiformis* polysaccharide with wound healing activity (Veeraperumal et al., 2020), *Saccharina japonica* polysaccharide with anti-inflammatory activity (Ni et al., 2020), non-digestible polysaccharides with anti-obesity effect (Lin, Zhang, Li, Zheng, & Hu, 2021; Zhang, Xie, You, Cheung, & Zhao, 2021)), and fucoidan extracted from brown algae, which exert anti-cancer activity (Oliveira, Neves, Reis, Martins, & Silva, 2020). In-depth investigation on marine alga polysaccharides with biological activities can provide novel insights for the treatment of diseases, and also as functional food.

Caulerpa chemnitzia (original name was *Caulerpa racemosa* var. *pel-tata*), a species of green syphonous algae of the genus *Caulerpa*, is widely distributed in semi-tropical and tropical regions. Polysaccharide is one

* Corresponding author.

E-mail addresses: danielwu@stu.scau.edu.cn (Y. Wu), lj2388240@gdmu.edu.cn (J. Liu), hhlhaohuili@stu.scau.edu.cn (H. Hao), hulianmei@scau.edu.cn (L. Hu), zhangxiaoyong@scau.edu.cn (X. Zhang), luolianxiang321@gdmu.edu.cn (L. Luo), zengjc@gdmu.edu.cn (J. Zeng), wzhang@must.edu.mo (W. Zhang), inwong@must.edu.mo (I. Nam Wong), huangriming@scau.edu.cn (R. Huang).

¹ First authors.

<https://doi.org/10.1016/j.fochx.2022.100313>

Received 22 July 2021; Received in revised form 7 April 2022; Accepted 15 April 2022

Available online 19 April 2022

2590-1575/© 2022 The Author(s). Published by Elsevier Ltd. This is an open access article under the CC BY-NC-ND license (<http://creativecommons.org/licenses/by-nc-nd/4.0/>).

of the main nutrient components of *Caulerpa chemnitzia*. Previous studies have displayed that *Caulerpa* polysaccharides have various biological activities such as *C. cylindracea* polysaccharide with anti-herpetic (Magdugo et al., 2020) and anti-inflammatory activities (Ribeiro et al., 2020), *C. lentillifera* polysaccharide with α -glucosidase inhibitory (Chaiklahan, Srinorasing, Chirasuwan, Tamtin, & Bunnag, 2020) and antioxidant activities (Tian, Liu, Song, Zhu, & Yin, 2021), *C. cupressoides* var. *flabellate* polysaccharide with immunostimulating activity (Barbosa et al., 2020), and *C. sertularioides* polysaccharide with osteogenic activity (Chaves, de Sousa, Viana, Rocha, de Medeiros, & Moreira, 2019). There is investigation on immunomodulatory effect of *C. chemnitzia* polysaccharides on NK cells and T lymphocytes of mice (Shen, Wang, Guo, & Tuo, 2008). Given the variety of promising applications of different polysaccharides from other species of the genus *Caulerpa*, this study aims to test for the potential immunomodulatory effects of a new polysaccharide isolated from *C. chemnitzia*.

In the study, extraction and purification of polysaccharide from *C. chemnitzia* was performed by hot-water extraction, ethanol precipitation and column chromatography. The physicochemical properties of *C. chemnitzia* polysaccharide were revealed by high-performance anion-exchange chromatography with pulsed amperometric detection (HPAEC-PAD), high-performance gel-permeation chromatography (HPGPC), Fourier transform-infrared spectroscopy (FT-IR) and gas chromatography-mass spectrometer (GC-MS). Meanwhile, in vitro immunomodulatory effect of polysaccharide extracted from *C. chemnitzia* was tested on RAW264.7 macrophages by measuring cell viability, nitric oxide (NO) production, and cytokines (TNF- α and IL-6) secretion. The molecular details of the immunostimulatory activity were analyzed through transcript-metabolite profiling.

Materials and methods

Materials and reagents

C. chemnitzia was collected from an area off Zhanjiang, China, in April 2017. A voucher specimen (No. 20170408) was deposited in Guangdong Provincial Key Laboratory of Food Quality and Safety, South China Agricultural University, China. Murine macrophages RAW264.7 were obtained from Jinan University (Guangzhou, China). Lipopolysaccharide (LPS), Sephadex G-100 and DEAE-52 anion-exchange column were purchased from Shanghai Yuanye Bio-Technology Co. LTD (Shanghai, China). Arabinose (Ara), glucose (Glc), fucose (Fuc), galactose (Gal), mannose (Man), fructose (Fru), xylose (Xyl), ribose (Rib), glucuronic acid (GlcA) and galacturonic acid (GalA) were purchased from Sigma Co. (MO, USA). Penicillin-streptomycin, fetal bovine serum (FBS), phosphate buffer solution (PBS) and Dulbecco Modified Eagle Medium (DMEM) were purchased from Gibco Life Technologies (USA). Cell Counting Kit-8 (CCK-8 kit) and Nitric oxide (NO) kit were purchased from Beyotime Biotechnology Co. LTD and Dongren Chemical Technology Co. LTD, respectively. Murine IL-6 and TNF- α ELISA kits were purchased from NeoBioscience Biotechnology Co. LTD. This study made use of analytical grade chemicals exclusively.

Preparation of CCP

The extraction of polysaccharides from *C. chemnitzia* was performed following the published procedures but with some modifications, which included the ratio of algae powder to water, the temperature of extraction, and the proportion of anhydrous ethanol added (Seedeve et al., 2018; Zhang et al., 2014). The *C. chemnitzia* (100 g) powder was added in 3000 mL of water and the mixture was extracted at 85 °C for 3 h twice. A gauze (200 mesh) was used for the filtration of the extract. After filtration, the water-soluble extract was concentrated by a rotary evaporator to 5% of its original volume at 65 °C, then centrifuged for 10 min at 22,000 g. The deproteinization of the supernatant was carried out by the Sevage method with Sevage reagent (*n*-butanol: chloroform = 1: 4,

(v/v)) (Yang, Huang, Wang, Cao, & Sun, 2008). After centrifuged, the supernatant was treated with three times of its volumes with anhydrous ethanol for 24 h. The sediment was dissolved and then dialyzed with tap-water and deionized water for 2 days and 1 day with the cut-off of Mw 8000 Da respectively, and lyophilized to obtain crude polysaccharides by freeze-drying.

Deionized water was used for the dissolution of crude polysaccharides. The solution was added to a pre-equilibrated Cellulose DEAE-52 anion-exchange column (3 cm \times 40 cm) and then eluted stepwise by NaCl solutions at a flow rate of 1.0 mL/min from a low to a high concentration (0, 0.1, 0.3, 0.6, 0.9, and 1.2 M). The eluents were gathered (10 mL/tube) and detected by the phenol-sulfuric acid method at 490 nm (Masuko, Minami, Iwasaki, Majima, Nishimura, & Lee, 2005). The major eluted fraction was further subjected to a Sephadex G-100 size-exclusion column (3 cm \times 50 cm), eluting by ultrapure water at a flow rate of 25 mL/h to obtained CCP (eluted by 0.6 M NaCl solution) which was prepared for further study.

Physicochemical characterizations of CCP

Chemical analyses

We measured the total sugar content of CCP by phenol-sulfuric acid method (Masuko, Minami, Iwasaki, Majima, Nishimura, & Lee, 2005) with glucose as the standard and quantified the content of uronic acid by *m*-hydroxybiphenyl method (Xia, Liang, Yang, Wang, & Kuang, 2011) using glucuronic acid as the standard. The content of protein was measured by Bradford's method (Bradford, 1976) with bovine serum albumin as the standard. Sulfate content, with K₂SO₄ used as the standard, was determined by the barium chloride-gelatin method (Dodgson & Price, 1962).

UV and FT-IR analysis

CCP (500 μ g/mL) was analyzed in the wavelength range of 200–600 nm by an Evolution 300 UV-VIS spectrometer (Thermo Scientific) to detect the presence of nucleic acids and proteins. The organic function groups of CCP were identified in the spectrophotometer range of 4000–400 cm⁻¹ by FT-IR. CCP (1.5 \pm 0.5% mg) mixed with 100 mg of spectroscopic grade KBr powder was milled accurately, then pressed into a 1 mm pellet for FT-IR analysis via VERTEX 70 FT-IR infrared spectrometer (Bruker, Germany).

Molecular weight and monosaccharide composition determination

The molecular weight distribution was estimated by HPGPC equipped with a multi-angle laser light scattering photometer (MALLS) and a refractive index detector (RID). The system was equipped with Ohpak SB-804 HQ columns and Ohpak SB-806 HQ at a temperature of 60 °C. CCP (5 mg) was dissolved with mobile phase (1 mL) and filtered through 0.45 μ m membrane filters. Then, the sample (100 μ L) was added to the system. Mobile phase (0.4 mL/min) was 0.1 M NaNO₃ mixed with 0.02% NaN₃ solution.

HPAEC-PAD was used to determine the monosaccharide compositions of CCP (Ji, Zhang, Zhang, Liu, Peng, & Wang, 2019). The equipment consisted of an ICS-5000 system (Thermo Fisher Scientific) which equipped with Dionex™ CarboPac™ PA20 (150 mm \times 3 mm, 6.5 μ m) and a pulsed amperometric detector. CCP (5 mg), mixed with 1 mL of 2.5 M trifluoroacetic acid (TFA), was directly hydrolyzed for 2 h at 121 °C. After the hydrolysis, the redundant TFA was removed with nitrogen gas and methanol was added three times. The dried sample which dissolved in the deionized water was prepared for the injection to the system.

SEM analysis

The microstructures of CCP were characterized by a Zeiss scanning electron microscope (SEM) at a 5 kV accelerating voltage at three different image magnifications (500 \times , 1000 \times , and 2000 \times).

Immunostimulatory activity of CCP on macrophage RAW264.7 cells

Cell culture

The macrophage RAW264.7 cells were cultured in a humid incubator at 37 °C with 5% CO₂. The cell medium was DMEM supplemented with 1% (v/v) penicillin–streptomycin and 10% (v/v) FBS. Cells cultured in sterile tissue culture flasks were prepared for further study.

Assay of cell viability

We measured the RAW264.7 cell viability via a CCK-8 assay. RAW264.7 cells planted in 96-well plates (100 µL/well) with a density of 3.0×10^4 cells/mL were cultured in an incubator as above for 24 h. The concentrations of CCP placed in the well were 0, 10, 30, 60, 100, 200, 300, 400 and 500 µg/mL. After the treatment with CCP, RAW264.7 cells planted in 96-well plates were incubated for 24 h. After the incubation, 10 µL of CCK-8 solution was added to each well of the plates and incubated for 2 h. The absorbance at 450 nm of each well was measured with a microplate reader.

Assay of NO and cytokine production

RAW264.7 cells planted in 24-well plates (500 µL/well) with a density of 3.0×10^5 cells/mL were cultured in a humidified incubator as above for 24 h. After incubation, RAW264.7 cells were treated with LPS (1 µg/mL) or CCP (0, 10, 30, 50, and 80 µg/mL) and incubated for another 24 h. The NO production levels and IL-6 and TNF- α secretion in the supernatants that collected from each group were determined with ELISA kits.

Transcript-Metabolite profiling

Transcriptomic analysis

The transcriptomic analysis of the control and CCP treated groups of the macrophage RAW264.7 cells was carried out based on the published method (Han et al., 2020). RNA of the macrophage RAW264.7 cells were extracted with Trizol reagent and used to establish the transcript library and Illumina sequencing (3 replicates per group). The concentration and integrity of RNA were examined with NanoPhotometer spectrophotometer and Agilent 2100 bioanalyzer, respectively. The transcript library was established using NEBNext® Ultra™ RNA Library Prep Kit for Illumina®, then sequenced through Illumina platform to obtain the paired-end reads. Clean reads were obtained after filtration of the raw reads, using for the downstream procedures. Paired-end clean reads were assigned to the reference genome of the macrophage RAW264.7 cells by using HISAT2 (v2.0.5) for further differentially expressed genes (DEGs) analysis. Genes with $|\log_2(\text{foldchange})| > 0$ and an adjusted *p*-value (*padj*) < 0.05 were considered as DEGs.

Metabolite analysis

The metabolite analysis of the control and CCP treated groups of the macrophage RAW264.7 cells was performed in line with a standard metabolic operating procedure (Han et al., 2020). The samples (6 biological replicates in each group) mixed with methanol/acetonitrile (1:1, v/v) were homogenized for one minute, then centrifuged (12000 g) for 10 min at 4 °C and the supernatant was collected for analysis. The widely targeted metabolic profile of the extracts of the macrophage RAW264.7 cell was carried out by ultrahigh performance liquid chromatography-electrospray ionization-tandem mass spectrometry (UPLC-ESI-MS/MS) system (UPLC, Shim-pack UFLC SHI-MADZU CBM A system; MS, QTRAP® System). Orthogonal partial least-squares discriminant analysis (OPLS-DA) and Pareto-scaled principal component analysis (PCA) were applied to normalize the obtained metabolic data. Then, the assessment of variable importance in projection (VIP) value was performed based on the result of OPLS-DA. Metabolites with adjusted *p*-value < 0.05, fold change ≥ 2 or fold change ≤ 0.5 , and VIP ≥ 1 were regarded as differentially accumulated metabolites (DAMs).

Statistical analysis

The statistical analysis was performed on ANOVA (SPSS 19.0) at a nominal alpha-level of 0.05. The *p*-values were interpreted as a measure of the strength of the evidence against the null hypothesis, which regarded lack of differences between the experimental groups and the control one. A *p*-value < 0.05 or 0.001 was regarded as significant differences or extremely significant differences, respectively.

Results and discussion

Preparation and chemical composition of CCP

In the current study, crude *C. chemnitzia* polysaccharide, which the yield was about 1.5% (the ratio of crude polysaccharide weight to algae powder weight), was obtained from *C. chemnitzia* powder by hot-water extraction, deproteinization and ethanol precipitation. We separated the crude polysaccharide by a DEAE-52 anion-exchange column and obtained 5 fractions (Fig. 1A). It was awfully difficult to purify the other eluted fraction except the fractions eluted by 0.1 M NaCl solution (named CRVP-1) which had been published previously (Hao et al., 2019) and 0.6 M NaCl solution (named CCP). In this study, we concentrated on studying the physicochemical characterization and immunostimulatory activity of CCP. To obtain high-purity polysaccharides, CCP was run through a Sephadex G-100 column and the elution curve displayed a proportioned figure (Fig. 1B). The solution in tubes number 8 to 12 was collected and lyophilized. The total sugar, the uronic acids, and the sulfate contents of CCP were measured as $59.18\% \pm 0.57\%$, $36.75\% \pm 0.28\%$, and $42.50\% \pm 0.42\%$.

Physicochemical characterizations of CCP

Weak characteristic absorption had been shown at 280 and 260 nm in the UV spectrum (Fig. 1C) of CCP, indicating little existence of nucleic acid or protein. Meanwhile, the maximum absorbance peak around 199 nm indicated the presence of polysaccharides (Chen & Kan, 2018). The average molecular weight of CCP was 321.6 kDa detected by HPGPC (Fig. 1D).

FT-IR analysis

As the wavenumber changed, different absorption bands emerged in the FT-IR spectrum of CCP (Fig. 2A). Absorption bands were assigned in line with previous references (Chen & Kan, 2018; Yuan, Zhao, Cha, Sun, Ye, & Zeng, 2015) to structural different groups respectively. Typical signals of polysaccharides had been shown in the FT-IR spectrum of CCP. The broadband at 3464 cm^{-1} was attributed to the O—H stretching vibration. The band at 2939 cm^{-1} and 1381 cm^{-1} were assigned to C—H bending and stretching vibration, respectively. The band at 1641 cm^{-1} attributed to stretching vibration of C=O was the structural characterization of uronic acid. The band at 1256 cm^{-1} attributed to stretching vibration of O=S=O sulfate esters (Zhang et al., 2019). The peak at 815 cm^{-1} was assigned to the C—O—S vibration, which suggested that the sulfate groups were mainly at the C-3 position (Foley, Szegezdi, Mulloy, Samali, & Tuohy, 2011). The peaks at 1138 cm^{-1} , 1054 cm^{-1} , and 1025 cm^{-1} were attributed to the C—O—C and C—O—H stretching vibration. The absorption band around 1050 cm^{-1} indicated the existence of pyranose rings (Liang et al., 2019).

Monosaccharide composition analysis

Monosaccharide composition of CCP was analyzed by HPAEC-PAD. It was shown that the main monosaccharides of CCP were galactose (30.47%), glucose (30.61%), mannose (15.41%), and glucuronic acid (10.66%). CCP also consisted of fucose (4.94%), galacturonic acid (3.20%), arabinose (1.87%), xylose (1.45%), fructose (0.98%) and ribose (0.41%). Meanwhile, CRVP-1 was mainly composed of mannose (92.1%) and galactose (2.9%), indicating that CRVP-1 and CCP were

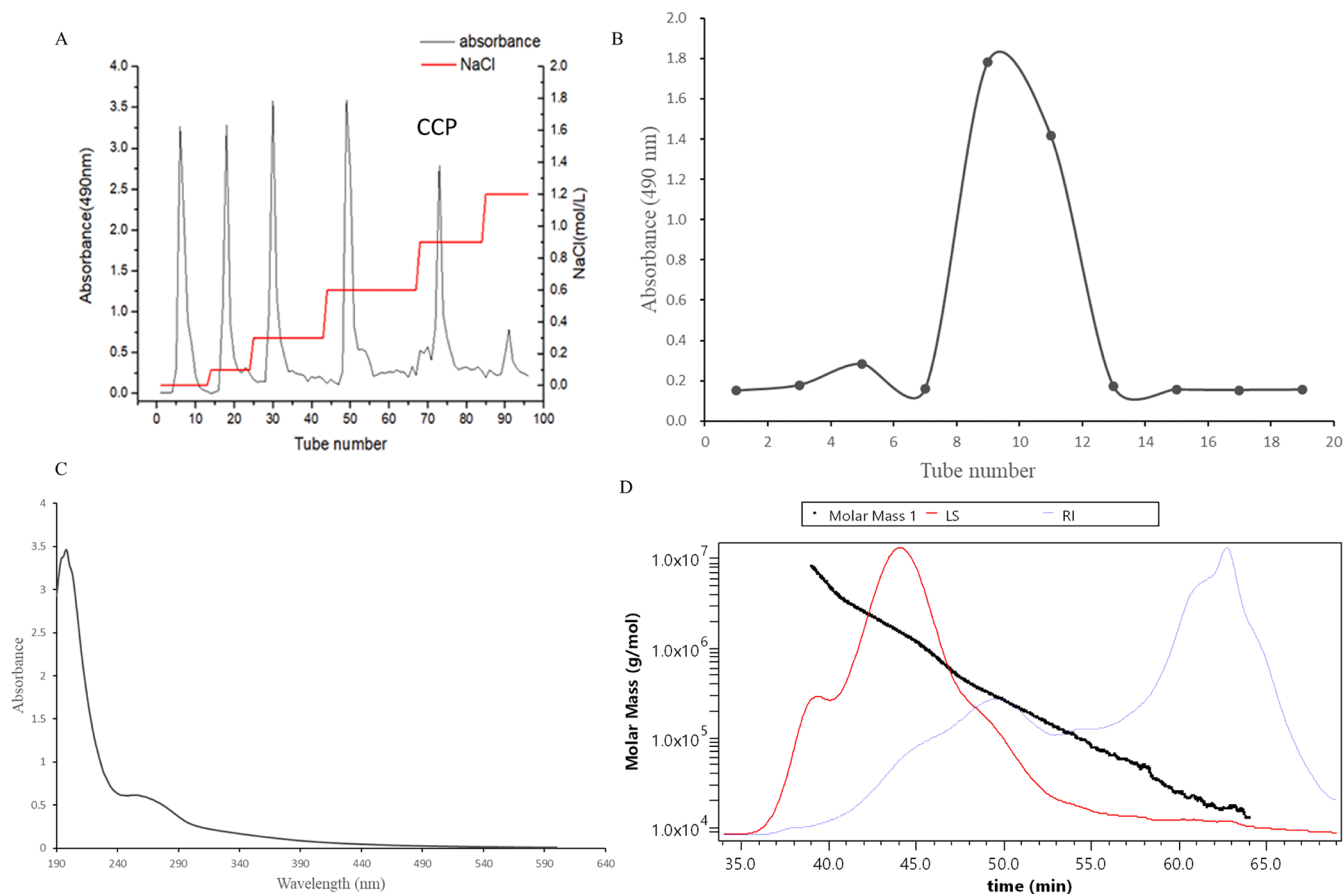


Fig. 1. (A) Elution curve of CCP on the DEAE-52 anion-exchange column. (B) Elution curve of CCP on a Sephadex G-100 column. (C) UV spectrum of CCP. (D) HPGPC profile of CCP.

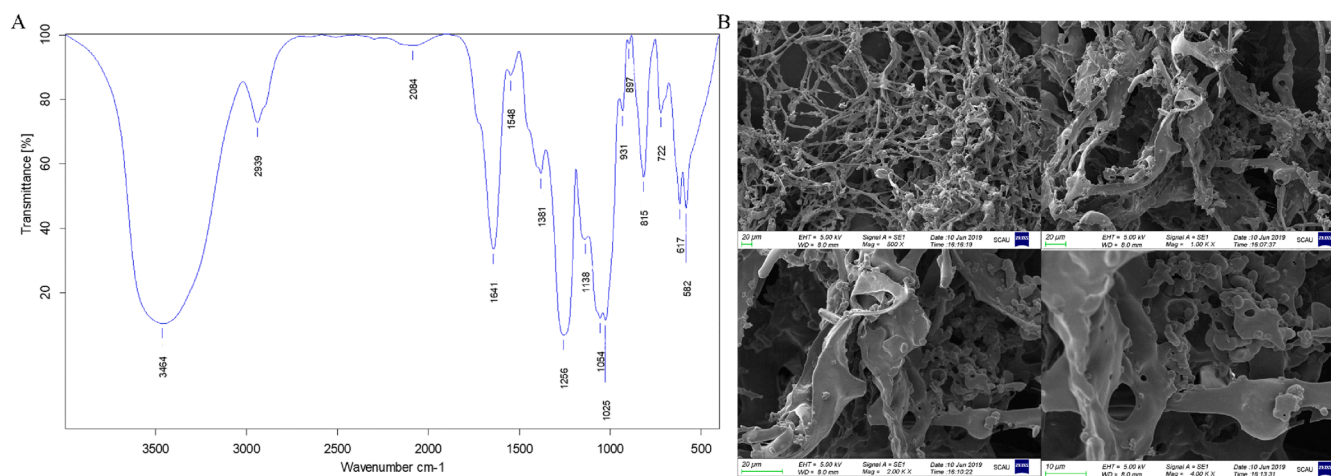


Fig. 2. (A) FT-IR spectrum of CCP. (B) The SEM morphological properties of CCP.

actually different polysaccharides.

SEM analysis

The morphological properties of CCP were observed by SEM (Fig. 2B) at magnifications of 500 ×, 1000 ×, and 2000 ×, respectively. It was shown that CCP had a complex and irregular surface microstructure. CCP was lamellate with slightly curved edges, indicating the presence of close connection and strong intermolecular interaction. The surface was not smooth but with holes and protrusions.

Immunomodulatory effect of CCP on RAW264.7 cells

Assessment of cell viability

The cytotoxicity of CCP was evaluated on RAW264.7 macrophages (Fig. 3A). Cell viability ratio across CCP concentrations presented an uptrend, revealing that CCP at the tested concentrations had no cytotoxicity on macrophages RAW264.7 and even promoted the proliferation of macrophage RAW264.7. This result was in line with that of CRVP-1. Cell viability presented a decreasing trend when the CCP concentration was higher than 300 μg/mL. The reason may be that

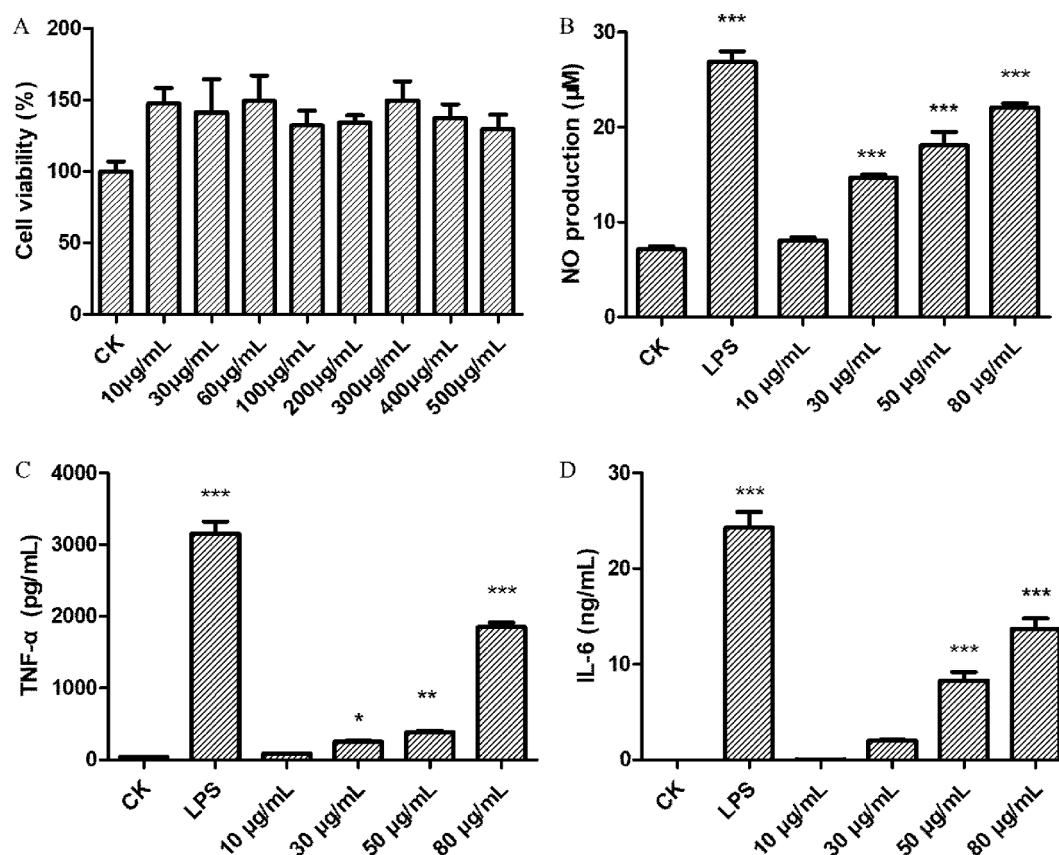


Fig. 3. (A) Effects of CCP on macrophages RAW264.7 proliferation. (B) Effects of CCP on NO production by macrophages RAW264.7. (C) Effects of CCP on secretion of TNF- α by macrophages RAW264.7. (D) Effects of CCP on secretion of IL-6 by macrophages RAW264.7. * denotes the differences between the control group and other groups, * $P < 0.05$, ** $P < 0.01$, and *** $P < 0.001$.

macrophages engaged in competition for CCP as nutritional resource following cell proliferation.

Determination of NO production

NO, considered as a product of L-arginine oxidation catalyzed by NO synthase, is an active molecule in various cells and plays an important role in cell inflammation response (Ma et al., 2020). NO production was measured in RAW264.7 macrophages after being treated with CCP at different concentrations (Fig. 3B). The effect of CCP at 10, 30, 50, and 80 $\mu\text{g/mL}$ on NO production by RAW264.7 macrophages was inferior to that of LPS on the same response variable when tested at 1 $\mu\text{g/mL}$. However, the relative effects of CCP on NO production were consistent and linearly related to the dosage. In addition, CCP with tested concentration performed better on promoting NO production than CRVP-1.

Measurement of cytokine production

The effect of CCP on stimulating cytokines (TNF- α and IL-6) released from macrophages RAW264.7 cells was dose-dependent. Secretion of TNF- α displayed an exponential trend at increased dosages (Fig. 3C). In contrast, the trend of IL-6 secretion was roughly linear (Fig. 3D). The present findings indicate that CCP trigger an immune response in RAW264.7 macrophages. Compared with the control groups, low dosage CCP treated groups (10 and 30 $\mu\text{g/mL}$) displayed little significant influence on macrophages RAW264.7 cells but the high dosage CCP treated groups (50 and 80 $\mu\text{g/mL}$) showed a highly significant effect. The above results showed that CCP could stimulate cytokines secretion of macrophages RAW264.7 cells, suggesting CCP may play a role in an immune response.

Transcript-Metabolite profiling of macrophages RAW264.7 treated with CCP

Transcriptomic analysis

A transcriptomic analysis was carried out to reveal the differences in RNA transcription rates on RAW264.7 macrophages between CCP treated and control groups. Genes detected in the control and CCP-treated groups with an adjusted p -value ($padj$) < 0.05 and $|\log_2(\text{foldchange})| > 0$ were considered as DEGs. 7692 genes were DEGs, including 3938 up-regulated and 3754 down-regulated genes (Fig. 4A). Gene ontology (GO) reflects the properties of genes and their products from 3 aspects, including molecular function (MF), cellular component (CC) and biological process (BP). Hence GO analysis of DEGs was carried on to unveil the gene changes of RAW264.7 macrophages responded to CCP (Fig. 4B). It was shown that most up-regulated DEGs were present in CC and BP (Fig. 4C), especially in BP. Most of the down-regulated were present in BP and CC as well, but mostly in CC (Fig. 4D). The DEGs enrichment suggested that CCP may influence the biological process and cellular components to exert an immunomodulatory effect. In BP categories, the most significant terms were "cell division" and "regulation of cell cycle process". In CC categories, the most significant terms were "chromosome, centromeric region" and "chromosomal region". In MF categories, the most significant terms were "enzyme activator activity" and "chromatin binding".

Kyoto encyclopedia of genes and genomes (KEGG) analysis was carried out for DEGs to understand the transcriptomic changes in the pathways. 29 pathways were enriched ($padj < 0.05$), in which "NOD-like receptor signaling pathway", "NF- κB signaling pathway", "Toll-like receptor signaling pathway" and "IL-17 signaling pathway" were related to the immunomodulatory effect. 20 pathways with the most significant enrichment were shown in Fig. 4E.

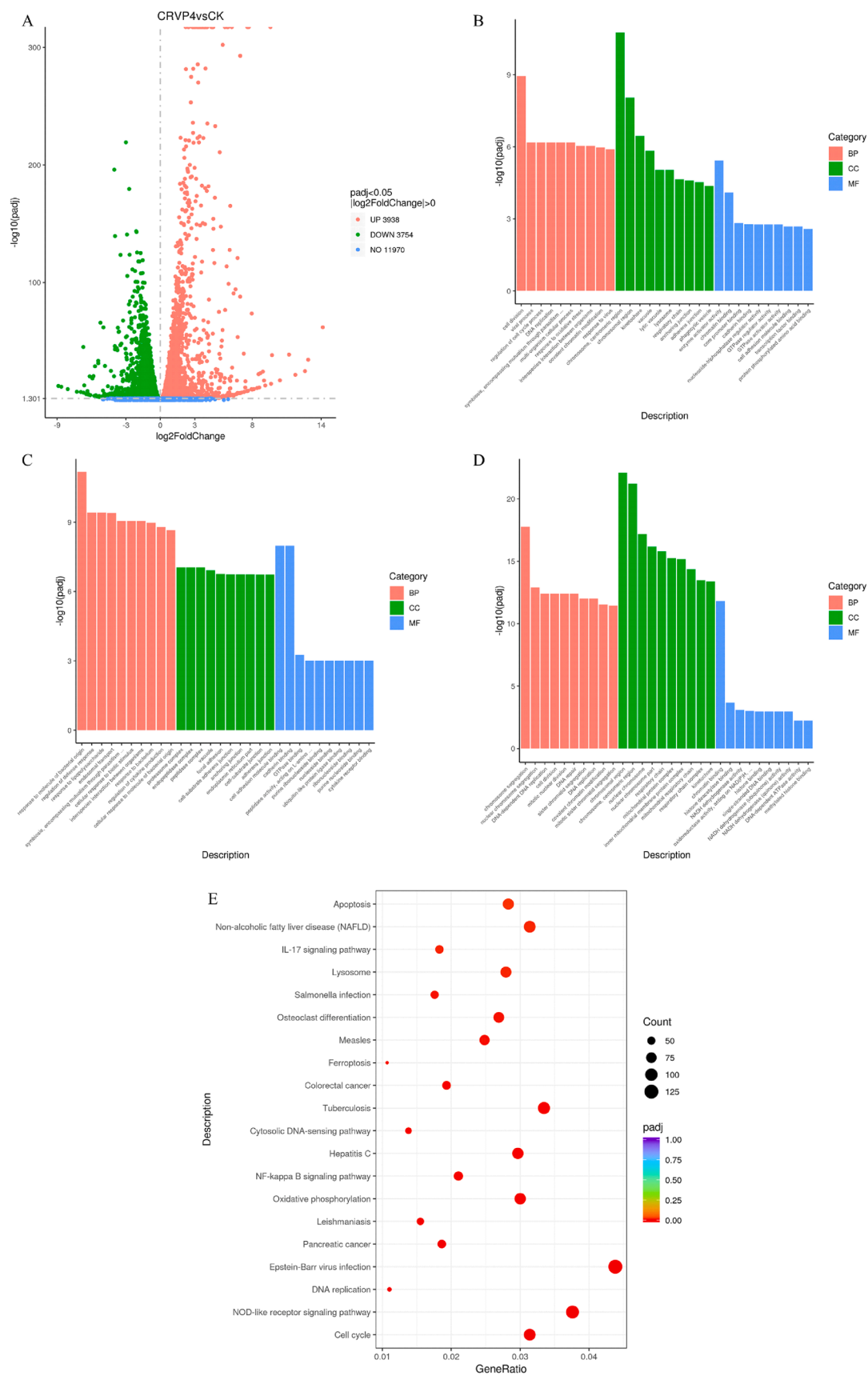


Fig. 4. (A) The volcano plot of DEGs. (B) GO analysis of DEGs. (C) GO analysis of up-regulated DEGs. (D) GO analysis of down-regulated DEGs. (E) TOP 20 of KEGG enrichment analysis for DEGs. The circle size reflects the amount of DEGs related to the pathways, and the circle color reflects the *padj* value of pathways.

Metabolomic analysis

We analyzed the extracts of macrophages RAW264.7 treated with CCP and the control groups by a UPLC-ESI-MS/MS system. The data were analyzed via PCA and OPLS-DA to evaluate the technical variation (Figure S1-S4). The result revealed that there were 95 DAMs which included 41 up-regulated and 54 down-regulated metabolites in RAW264.7 macrophages between CCP treated group and the control group (Table S1, Fig. 5A). Glycyl-L-proline, glycochenodeoxycholic acid, dulcitol, succinic acid, α -ketoglutaric acid, D-sorbitol and so on were significantly up-regulated while L-threonine, L-aspartic acid, L-serine, β -Alanine, adenosine 5'-monophosphate, uridine 5'-diphospho-N-acetylgalactosamine and so on were significantly down-regulated. The different metabolites belonged to 5 main groups included amino acid, lipid, carbohydrate, nucleotide, and organic acid.

KEGG for DAMs was carried out and 15 pathways were enriched ($P < 0.05$). Pathways related to carbohydrate metabolism were "galactose metabolism", "starch and sucrose metabolism", and "glycolysis/gluconeogenesis". Pathways involved in amino acid metabolism were "lysine degradation", "glycine, serine, threonine metabolism", and " β -alanine metabolism". Arachidonic acid metabolism was related to lipid metabolism. 20 pathways with the most significant enrichment, including "arachidonic acid metabolism" and "galactose metabolism" were shown in Fig. 5B. DAMs involved in arachidonic acid metabolism were 15-deoxy- δ -12, 14-PGJ₂, TXB₂, 15-oxo-5Z,8Z,11Z,13E-eicosatetraenoic acid, PGD₂, PGJ₂, and PGE₂, all of which were significantly up-regulated. DAMs related to the galactose metabolism were UDP-glucose, myoinositol, dulcitol, D-sorbitol and D-glucose, with D-sorbitol and dulcitol being significantly up-regulated, while the others were significantly down-regulated.

Transcript-metabolite analysis

To analyze the properties and relationship of DAMs and DEGs which appeared enriched in the macrophage RAW264.7 cell exposed to CCP, the correlation network was established, including correlation pairs associated with the functionally annotated signaling pathways (Fig. 6). Nine pathways that both enriched in transcriptomic and metabolomic, including galactose metabolism pathway, glycolysis/ gluconeogenesis pathway, glycine, serine and threonine metabolism pathway, lysine degradation, inositol phosphate metabolism pathway, propanoate metabolism, glucagon signaling pathway, HIF-1 signaling pathway and central carbon metabolism in cancer pathway. In order to explain the possible mechanism of the immunomodulatory effect of CCP on

macrophages and the relationship between DAMs and DEGs, the pathways related to the immune response were selected for further analysis.

Since NF- κ B signaling pathway plays an important role in immune response of cells, we focused on the changes in this signaling pathway and found that there were 61 DEGs, which included 39 up-regulated DEGs and 22 down-regulated ones. Under the normal conditions, NF- κ B is present in the cytoplasm in the form of inactivated p50/p65/I κ B α trimer. When exposed to external stimulation, the phosphorylation and ubiquitination of I κ B protein occur and subsequent degradation to dissociate from p50/p65. The dissociative I κ B protein is then transferred to the cell nucleus and combined with the promoter regions of target genes (such as TNF- α and IL-1 β , etc.) to initiate gene transcription, and thus exert an immunostimulatory activity (D. Z. Shen, Xin, Chen, & Liu, 2013). The results revealed that p50, I κ B α and cyclooxygenase 2 (COX-2) were upregulated in the genes level (Figure S5) after the CCP treatment. The up-regulation of I κ B α in gene level revealed that the pathway had been activated by CCP and the phosphorylation, ubiquitination and degradation of I κ B α might occur. CCP treatment upregulated the expression of p50 at gene level, thereby further increasing the expression of cytokines such as TNF- α and IL-1 β at gene level, ultimately promoted the secretion of cytokines. As CCP played an immunostimulatory role by activating the macrophages to promote the phosphorylation of I κ B and p65, increasing the cytokines expression, and inducing the macrophages phenotype conversion (Liu, Zhang, Joo, & Sun, 2017). Meanwhile, attention was paid to the changes in mitogen-activated protein kinases (MAPK) signaling pathway. MAPK is a key factor of innate and adaptive immune response, and MAPK signaling pathway consists of extraneous signal-regulated kinase (ERK) signaling pathway, c-Jun N-terminal kinase (JNK) signaling pathway and p38 mitogen-activated protein kinase (p38) signaling pathway. The results revealed that CCP up-regulated the expression of MAPKs included ERK, JNK and p38 at the gene level (Figure S6), and these MAPKs are activated by phosphorylation. These changes might promote macrophages proliferation and differentiation, cause inflammatory response and apoptosis, and take part in modulating the cytokines secretion (Wang, Wei, Yue, Wu, Wang, & Zhang, 2021). In brief, the obtained results indicated that CCP might play an immunostimulatory role by activating NF- κ B signaling pathway, and promote macrophage proliferation by activating MAPK signaling pathway to further prompt immune response.

Arachidonic acid (AA), the ω -6 polyunsaturated fatty acid, and its metabolism pathway have attracted the attention of researchers in immune processes and diseases (Capra et al., 2013; Wang et al., 2021). AA

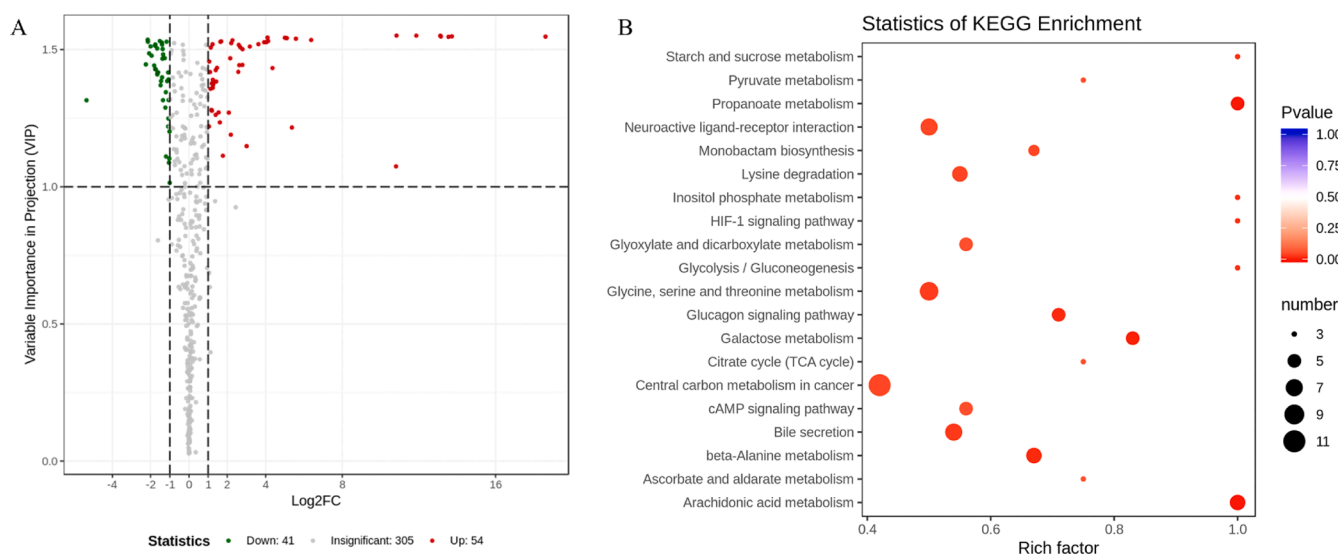


Fig. 5. (A) The volcano plot of DAMs. (B) TOP 20 of KEGG enrichment analysis for DAMs. The circle size reflects the amount of DAMs related to the pathways, and the circle color reflects the p -value of pathways.

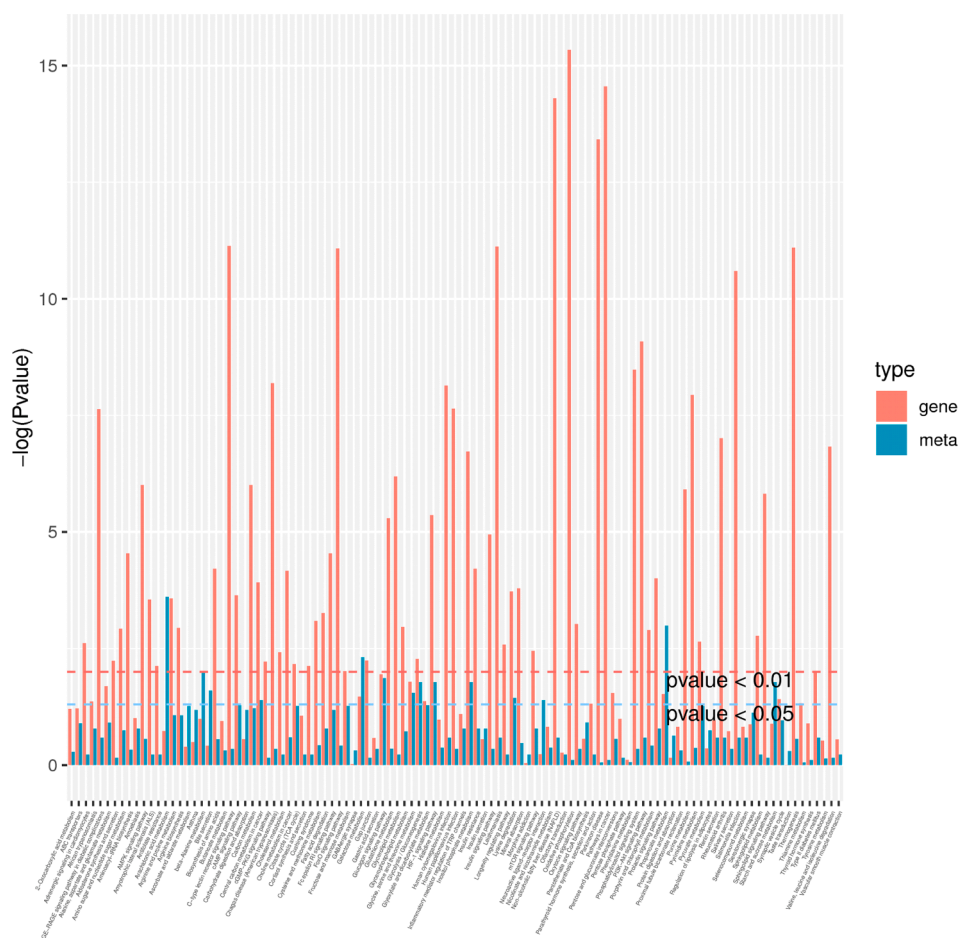


Fig. 6. KEGG pathways that both enriched in transcriptomic and metabolomic of the macrophages RAW264.7 treated with CCP.

can be metabolized by three different enzyme systems including cytochrome P450 (CYP) enzymes, lipoxygenases (LOXs) and cyclooxygenases (COXs). Phospholipase A2 (PLA2) catalyzes the change of esterified AA on the cell membrane to its free form. Free AA is further metabolized by COXs to unstable endoperoxide including PGG₂ and PGH₂ (Wang et al., 2021) which is also catalyzed by terminal synthase enzymes included prostaglandin E (PGE) and PGD synthases to produce PGE₂ and PGD₂. We found that there were 17 DEGs, including 7 up-regulated and 10 down-regulated DEGs, in arachidonic acid metabolism pathways following the CCP treatment. The results also revealed that there were 6 DAMs in the pathway including PGE₂, PGD₂, TXB₂ and so on. COXs are limiting factors of PGs synthesis. CCP increased the expression of COXs especially COX-2 in the gene level, and thus leading to the accumulation of PGE₂ and PGD₂ (Figure S7). PGE₂ plays an important role in immune response and it stimulates secretion of cytokines (such as TNF- α and IL-6) which regulates the innate immunity (Monmai et al., 2020). PGE₂ can also exert an immunomodulatory effect by promoting macrophages phenotype conversion and by modulating regulatory T cells development and function (AN et al., 2018). In addition, PGD₂ can be a key mediator for fungicidal and phagocytosis functions of macrophages (Pereira et al., 2018). Therefore, it is speculated that CCP may cause the accumulation of PGE₂ by activating the arachidonic acid metabolism pathway, and might play an immunostimulatory role through its effects on PGE₂, cytokines, and regulatory T cells.

Conclusion

Caulerpa chemnitzia can be farmed with simple condition and low

cost. The polysaccharide of *Caulerpa chemnitzia* can be obtained easily and can become a standard source for study and application on functional foods. Investigation on *Caulerpa chemnitzia* polysaccharides led to the isolation and characterization a new polysaccharide (CCP) with a molecular weight of 321.6 KDa. The basic components of CCP were the total sugar content ($59.18\% \pm 0.57\%$), the uronic acids content ($36.75\% \pm 0.28\%$), and the sulfate content ($42.50\% \pm 0.42\%$). The heteropolysaccharide CCP was composed of arabinose, fucose, glucose, galactose, mannose, xylose, fructose, ribose, glucuronic acid, and galacturonic acid with rates of 1.87%, 4.94%, 30.61%, 30.47%, 15.41%, 1.45%, 0.98%, 0.41%, 10.66%, and 3.20%, respectively. Immunostimulatory assay showed that CCP increases cell viability, production of nitric oxide, and secretion of cytokines (IL-6 and TNF- α). Transcript-metabolite outcome of macrophage RAW264.7 exposed to CCP displayed a total of 7692 DEGs (3938 up-regulated and 3754 down-regulated ones) and a total of 95 DAMs (41 up-regulated and 54 down-regulated ones). The transcript-metabolite analysis indicated that CCP exerts an immunomodulatory effect on RAW264.7 by activating the NF- κ B signaling pathway, and the arachidonic acid metabolism pathway. The provided findings of CCP will provide the basis for further investigation on the possible immunostimulatory mechanisms of *Caulerpa* polysaccharides.

Declaration of Competing Interest

The authors declare that they have no known competing financial interests or personal relationships that could have appeared to influence the work reported in this paper.

Acknowledgements

This work was financially supported by the National Natural Science Foundation of China (No. 32161160304), the Macao Science and Technology Development Fund (No. 0069/2021/AFJ), Key-Area Research and Development Program of Guangdong Province (No. 2020B1111030004), Program of Department of Natural Resources of Guangdong Province (No. GDNRC[2021]53), General project of Guangdong Medical Science and Technology Research Foundation (NO. A2021207), Characteristic innovation project of colleges and universities in Guangdong Province (NO. 2020KTSCX041); Finance Special Project of Zhanjiang City (NO. 2021A05095), Discipline construction project of Guangdong Medical University (NO. 4SG21279P).

Appendix A. Supplementary data

Supplementary data to this article can be found online at <https://doi.org/10.1016/j.fochx.2022.100313>.

References

- AN, J. H., SONG, W. J., LI, Q., KIM, S. M., YANG, J. I., RYU, M. O., ... YOUN, H. Y. (2018). Prostaglandin E2 secreted from feline adipose tissue-derived mesenchymal stem cells alleviate DSS-induced colitis by increasing regulatory T cells in mice. *BMC Vet. Res.*, *14*, Article 354.
- Barbosa, J. D., Sabry, D. A., Silva, C. H. F., Gomes, D. L., Santana, A. P., Sasaki, G. L., & Rocha, H. A. O. (2020). Immunomodulatory effect of Sulfated Galactans from the Green Seaweed *Caulerpa cupressoides* var. *flabellata*. *Mar. Drugs*, *18*, 234.
- Bradford, M. M. (1976). A rapid and sensitive method for the quantitation of microgram quantities of protein utilizing the principle of protein-dye binding. *Anal. Biochem.*, *72*, 248–254.
- Capra, V., Bäck, M., Barbieri, S. S., Camera, M., Tremoli, E., & Rovati, G. E. (2013). Eicosanoids and Their Drugs in Cardiovascular Diseases: Focus on Atherosclerosis and Stroke. *Med. Res. Rev.*, *33*, 364–438.
- Chaiklahan, R., Srinorasing, T., Chirasuwan, N., Tamtin, M., & Bunnag, B. (2020). The potential of polysaccharide extracts from *Caulerpa lentillifera* waste. *Int. J. Biol. Macromol.*, *161*, 1021–1028.
- Chaves, G. P., de Sousa, A. F. G., Viana, R. L. S., Rocha, H. A. O., de Medeiros, S. R. B., & Moreira, S. M. G. (2019). Osteogenic activity of non-genotoxic sulfated polysaccharides from the green seaweed *Caulerpa sertularioides*. *Algal. Res.*, *42*, Article 101546.
- Chen, G., & Kan, J. (2018). Characterization of a novel polysaccharide isolated from *Rosa roxburghii* Tratt fruit and assessment of its antioxidant in vitro and in vivo. *Int. J. Biol. Macromol.*, *107*, 166–174.
- Chi, Y., Zhang, M., Wang, X., Fu, X., Guan, H., & Wang, P. (2020). Ulvan lyase assisted structural characterization of ulvan from *Ulva pertusa* and its antiviral activity against vesicular stomatitis virus. *Int. J. Biol. Macromol.*, *157*, 75–82.
- Dodgson, K. S., & Price, R. G. (1962). A note on the determination of the ester sulphate content of sulphated polysaccharides. *Biochem. J.*, *84*, 106–110.
- Foley, S. A., Szegezdi, E., Mulloy, B., Samali, A., & Tuohy, M. G. (2011). An unfractionated fucoidan from *Ascophyllum nodosum*: Extraction, characterization, and apoptotic effects in vitro. *J. Nat. Prod.*, *74*, 1851–1861.
- Gong, G., Dang, T., Fang, J., Deng, Y., Liu, Q., Dai, W., ... Wang, Z. (2020). Preparation, structural characterization, and bioactivity of PHPD-IV-4 derived from *Porphyrha haitanensis*. *Food Chem.*, *329*, 127042.
- Han, Y., Wu, Y. L., Li, G. Q., Li, M. Y., Yan, R., Xu, Z. L., ... Huang, R. M. (2020). Structural characterization and transcript-metabolite correlation network of immunostimulatory effects of sulfated polysaccharides from green alga *Ulva pertusa*. *Food Chem.*, *342*, Article 128537.
- Hao, H. L., Han, Y., Yang, L. H., Hu, L. M., Duan, X. W., Yang, X., & Huang, R. M. (2019). Structural characterization and immunostimulatory activity of a novel polysaccharide from green alga *Caulerpa racemosa* var. *peltata*. *Int. J. Biol. Macromol.*, *134*, 891–900.
- Ji, X. L., Zhang, F., Zhang, R., Liu, F., Peng, Q., & Wang, M. (2019). An acidic polysaccharide from *Ziziphus Jujuba* cv. *Muzao*: Purification and structural characterization. *Food Chem.*, *274*, 494–499.
- Liang, X. X., Gao, Y. Y., Pan, Y., Zou, Y. F., He, M., He, C. L., ... Lv, C. (2019). Purification, chemical characterization and antioxidant activities of polysaccharides isolated from *Mycena dendrobii*. *Carbohydr. Polym.*, *203*, 45–51.
- Lin, H. T., Zhang, J. W., Li, S. Y., Zheng, B. D., & Hu, J. M. (2021). Polysaccharides isolated from *Laminaria japonica* attenuates gestational diabetes mellitus by regulating the gut microbiota in mice. *Food Frontiers*, *2*(2), 208–217.
- Liu, T., Zhang, L. Y., Joo, D. Y., & Sun, S. C. (2017). NF-κB signaling in inflammation. *Signal Transduct. Tar.*, *2*, 17023.
- Ma, G. X., Kimatu, B. M., Yang, W. J., Pei, F., Zhao, L. Y., Du, H. J., ... Xiao, H. (2020). Preparation of newly identified polysaccharide from *Pleurotus eryngium* and its anti-inflammation activities potential. *J. Food Sci.*, *85*, 2822–2831.
- Magdugo, R. P., Terme, N., Lang, M., Pliego-Cortes, H., Marty, C., Hurtado, A. Q., ... Bourgougnon, N. (2020). An analysis of the nutritional and health values of *Caulerpa racemosa* (Forsskal) and *Ulva fasciata* (Delile)-two chlorophyta collected from the Philippines. *Molecules*, *25*, Article 2901.
- Masuko, T., Minami, A., Iwasaki, N., Majima, T., Nishimura, S. I., & Lee, Y. C. (2005). Carbohydrate analysis by a phenol-sulfuric acid method in microplate format. *Anal. Biochem.*, *339*, 69–72.
- Monmai, C., Jang, A. Y., Kim, J. E., Lee, S. M., You, S. G., Kang, S. B., & Park, W. J. (2020). Immunomodulatory activities of body wall fatty acids extracted from *Halocynthia aurantium* on RAW264.7 cells. *J. Microbiol. Biotechnol.*, *30*, 1927–1936.
- Ni, L. Y., Wang, L., Fu, X. T., Duan, D. L., Jeon, Y. J., Xu, J. C., & Gao, X. (2020). In vitro and in vivo anti-inflammatory activities of a fucose-rich fucoidan isolated from *Saccharina japonica*. *Int. J. Biol. Macromol.*, *156*, 717–729.
- Oliveira, C., Neves, N. M., Reis, R. L., Martins, A., & Silva, T. H. (2020). A review on fucoidan antitumor strategies: From a biological active agent to a structural component of fucoidan-based systems. *Carbohydr. Polym.*, *239*, Article 116131.
- Pereira, P. A. T., Assis, P. A., Prado, M. K. B., Ramos, S. G., Aronoff, D. M., de Paula-Silva, F. W. G., ... Faccioli, L. H. (2018). Prostaglandins D2 and E2 have opposite effects on alveolar macrophages infected with *Histoplasma capsulatum*. *J. Lipid Res.*, *59*, 195–206.
- Qin, L., He, M. J., Yang, Y. J., Fu, Z. T., Tang, C. C., Shao, Z. L., ... Mao, W. J. (2020). Anticoagulant-active sulfated arabinogalactan from *Chaetomorpha linum*: Structural characterization and action on coagulation factors. *Carbohydr. Polym.*, *242*, Article 116394.
- Ribeiro, N. A., Chaves, H. V., da Conceição Rivanor, R. L., do Val, D. R., de Assis, E. L., Silveira, F. D., ... Benevides, N. M. B. (2020). Sulfated polysaccharide from the green marine algae *Caulerpa racemosa* reduces experimental pain in the rat temporomandibular joint. *Int. J. Biol. Macromol.*, *150*, 253–260.
- Seedeivi, P., Moovendhan, M., Sudharsan, S., Sivasankar, P., Sivakumar, L., Vairamani, S., & Shanmugam, A. (2018). Isolation and chemical characteristics of rhamnose enriched polysaccharide from *Grateloupia lithophila*. *Carbohydr. Polym.*, *195*, 486–494.
- Shen, D. Z., Xin, S. L., Chen, C., & Liu, T. (2013). Effect of atorvastatin on expression of TLR4 and NF-κB p65 in atherosclerotic rabbits. *Asian Pac. J. Trop. Med.*, *6*, 493–496.
- Shen, W. Z., Wang, H., Guo, G. Q., & Tuo, J. J. (2008). Immunomodulatory effects of *Caulerpa racemosa* var. *peltata* polysaccharide and its selenizing product on T lymphocytes and NK cells in mice. *Sci. China Series C-Life Sci.*, *51*, 795–801.
- Tian, H., Liu, H. F., Song, W. K., Zhu, L., & Yin, X. Q. (2021). Polysaccharide from *Caulerpa lentillifera*: Extraction optimization with response surface methodology, structure and antioxidant activities. *Nat. Prod. Res.*, *35*, 3417–3425.
- Veeraperumal, S., Qiu, H. M., Zeng, S. S., Yao, W. Z., Wang, B. P., Liu, Y., & Cheong, K. L. (2020). Polysaccharides from *Gracilaria lemaneiformis* promote the HaCaT keratinocytes wound healing by polarised and directional cell migration. *Carbohydr. Polym.*, *241*, Article 116310.
- Wang, B., Wu, L. J., Chen, J., Dong, L. L., Chen, C., Wen, Z., ... Wang, D. W. (2021). Metabolism pathways of arachidonic acids: Mechanisms and potential therapeutic targets. *Signal Transduct. Tar.*, *6*, Article 94.
- Wang, Q. C., Wei, M. S., Yue, Y., Wu, N., Wang, J., & Zhang, Q. B. (2021). Structural characterization and immunostimulatory activity in vitro of a glycogen from sea urchin-Strongylocentrotus intermedius. *Carbohydr. Polym.*, *258*, Article 117701.
- Xia, Y. G., Liang, J., Yang, B. Y., Wang, Q. H., & Kuang, H. X. (2011). A new method for quantitative determination of two uronic acids by CZE with direct UV detection. *Biomed. Chromatogr.*, *25*, 1030–1037.
- Yang, L. Y., Huang, L. J., Wang, Z. F., Cao, C. Y., & Sun, W. J. (2008). Isolation and purification and structural characterization of acidic polysaccharide FCP5-A from fruit of *Cornus officinalis*. *Chem. J. Chinese U.*, *29*, 936–940.
- Yuan, Q. X., Zhao, L. Y., Cha, Q. Q., Sun, Y., Ye, H., & Zeng, X. X. (2015). Structural characterization and immunostimulatory activity of a homogeneous polysaccharide from *Sinonovacula constricta*. *J. Agr. Food Chem.*, *63*, 7986–7994.
- Zhang, H. L., Cui, S. H., Zha, X. Q., Bansal, V., Xue, L., Li, X. L., ... Luo, J. P. (2014). Jellyfish skin polysaccharides: Extraction and inhibitory activity on macrophage-derived foam cell formation. *Carbohydr. Polym.*, *106*, 393–402.
- Zhang, Y. J., Xie, Q. T., You, L. J., Cheung, P. C. K., & Zhao, Z. G. (2021). Behavior of non-digestible polysaccharides in gastrointestinal tract: a mechanistic review of its anti-obesity effect. *eFood*, *2*, 59–72.
- Zhang, Z. Y., Wang, H., Chen, T. T., Zhang, H., Liang, J. Y., Kong, W. B., ... Wang, J. L. (2019). Synthesis and structure characterization of sulfated galactomannan from fenugreek gum. *Int. J. Biol. Macromol.*, *125*, 1184–1191.
- Zhao, C., Lin, G. P., Wu, D. S., Liu, D., You, L. J., Högger, P., ... Xiao, J. B. (2020). The algal polysaccharide ulvan suppresses growth of hepatoma cells. *Food Frontiers*, *1*, 83–101.